The Journal of Engine Research

Winter 2024, Vol. 70, No. 4, pp. 27-39

Journal Homepage: www.engineresearch.ir

Original Research

Characterization of High-pressure Hydrogen Jet for ICE in terms of Morphology and Flow-rates

Alessandro Montanaro*, Luigi Allocca, Giovanni Meccariello

Institute of STEMS–CNR, Italy

ARTICLE INFO

Keywords:
Hydrogen Injection
Direct Injection
Gaseous Fuel

ABSTRACT

The combustion of fossil-based fuels in ICEs, resulting in a huge amount of greenhouse gases (GHG) and leading to an immense global temperature rise, are the root causes of the more stringent emission legislations to safeguard health and that encourage further investigations on alternative carbon-neutral fuels. In this respect, the hydrogen has been considered as one of the potential clean fuels because of its zero-carbon nature. The current development of hydrogen-based ICEs focuses on the direct injection (DI) strategy as it allows better engine efficiency than the port fuel injection one. The behavior of the fuel jet is a fundamental aspect of the in-cylinder air-fuel mixing ratio, affecting the combustion process, the engine performances, and the pollutants emissions.In the present study, comprehensive investigations on the hydrogen jet behavior, generated by a Compressed Hydrogen Gas (CHG) injector under different operative conditions, were performed. A measuring system, suitable for the gaseous fuels, was used for measuring the flow rate. The fuel jet morphology was studied in a constant volume vessel filled with nitrogen as function of the injection pressure (up to 4.0 MPa) and different backpressure in the vessel, through the measurements of the jet penetrations, total areas, and cone angles showing a strong dependence from the set parameters. The cycle-resolved schlieren imaging technique by a high-speed camera was used to follow the jet spreads while the images were processed by a home-made procedure allowed to identify the contours of the hydrogen jet in the nitrogen gas and hence to measure the main parameters characterizing the jet structure.

* Corresponding author
E-mail address: alessandro.montanaro@stems.cnr.it (A. Montanaro)

Received 18 May 2024; Accepted 24 May 2024
E-ISSN: 2345-4121/ISSN: 1735-5214

Cite this article: Montanaro A, Allocca L, Meccariello G. Characterization of High-pressure Hydrogen Jet for ICE in terms of Morphology and Flow-rates. The Journal of Engine Research. 2024 Feb 20;70(4):27-39. doi: 10.22034/ER.2024.2029585.1054

1- Introduction

In addition to energy dependence issues, the environmental impact due to the combustion of fossil fuels remains the most critical issue. In particular, the transport sector is still responsible for about 25% of the European Union's (EU) Greenhouse gas emissions (GHG) direct emissions, while producing other pollutant emissions such as carbon monoxide (CO), nitrogen oxides (NOx) and particulate matter (PM) with strongly affect air quality and human health in urban spaces. According to decisions approved in 2020 at the European Green Deal, the target is to make the European Union climate-neutral in 2050 and to reduce GHG by 55% by 2030 [1]. Therefore, for the transition to net-zero emission in the transport sector, internal combustion engines (ICEs) powered by carbon-free fuels will play a key role. In this contest, hydrogen (H2) represents an attractive energy carrier for decarbonizing the transport sector, since it has the potential to address both GHG and pollutant emission problems [2-9]. H2 can be used in the transport sector both as a fuel for internal combustion engines and as an energy carrier for storing electricity possibly produced by renewable sources (green-H2) [10].

Hydrogen-fueled internal combustion engines (H2-ICEs) are gaining increasing interest for both light and heavy-duty applications since no carbon emissions are produced from its combustion process. Furthermore, hydrogen as a fuel in spark ignition engines can lead to reduced NOx emissions, if it is used in ultra-lean combustion strategies, potentially achievable thanks to its wide range of flammability and high lower heating value, auto-ignition temperature, flame speed, and Research Octane Number (RON > 130). Finally, H2-ICE technology can benefit from the reduced cost of using the existing mature manufacturing facilities and processes for conventional ICEs [11].

Despite the above advantages, the development of H2-ICEs is still in the conceptual and prototype stage, due to several drawbacks mainly related to the very low density of hydrogen. First, high storage pressure (from 350 up to 700 bar) is required to increase H2 density and ensure a proper vehicle range. Then, due to the low volumetric energy density of H2, the volumetric efficiency and the power density of the engine can be particularly penalized if the fuel is fumigated or injected into the intake manifold. Another issue associated with the hydrogen port injection is related to its small quenching distance and high laminar flame speed that imply a string propensity for flame backfiring in the intake manifold. Furthermore, despite the high RON and auto-ignition temperature giving H2 high knocking resistance, pre-ignition of the fuel during the compression stroke may occur. Indeed, the low minimum ignition energy of H2 at stoichiometric conditions could lead to the ignition of hot spots or residues in the cylinder.

The decrease in volumetric efficiency and the onset of abnormal combustion phenomena can be potentially solved by directly injecting H2 into the cylinder during the compression (at high pressure) or intake (at low-medium pressure) strokes, in the so-called direct injection (DI) engines [12-15]. The short time for the air-fuel mixing process in DI systems requires high hydrogen flow rates, so higher injection pressures compared to PFI. High injection pressures are also employed to ensure the accurate metering of the amount of fuel injected inside the combustion chamber [16, 17]. Indeed, when the injection pressure is greater than twice the back pressure, choking conditions are reached with consequent constant flow rates. Due to the possibility of different injection strategies and the variation of in-cylinder back-pressure, the comprehensive knowledge of hydrogen injection spray behavior and characteristics is fundamental for improving the combustion process in DI H2-ICE. The investigation of the spray macroscopic characteristics using optical techniques can provide, in fact, invaluable information on the mixture formation process. Experimental investigations on H2 injectors are also extremely useful for testing the injectors even before their assembly on the engine, helping to solve another problem typical of gaseous fuels, namely the lack of lubrication. Indeed, due to poor lubricating properties of H2, the injector could suffer from gas leakage inside the cylinder with

consequent abnormal combustion phenomena during engine cycles. The present work aims to deal the hydrogen jet behavior in terms of mass flow rate measurements and morphology investigation under a wide range of engine-like conditions. The spatial and temporal evolution of the H2 jet was studied by a z-type schlieren optical setup by injecting through a H2 injector into a constant volume combustion vessel (CVCV) as function of different injection and ambient pressures.

2- Experimental Background and Method

For the experimental campaign, hydrogen (99.999% purity), stored in a pressurized tank (200 bar initial pressure), was brought to the injector by a high-pressure single-stage regulator (maximum outlet pressure 100 bar), ensuring the desired value of injection pressure per each investigated condition. The gas was delivered through a PHINIA hydrogen pintle "outwardly opening" injector (DI-CHG10) equipped with a cap on the nozzle tip [18]. The injection system was carried out by a wide test campaign in terms of mass flow rate measurements and spatial/temporal jet characterization for different ambient and injection conditions.

2-1- Mass flow rate measurements

For the dynamic characterization of the injection system, it was necessary to create a special experimental apparatus, consisting of the gas supply line, the flow meter, and the electronics for managing the injector, phasing controlling, and acquiring the measurements. The layout of the experimental apparatus is schematically illustrated in Figure 1.

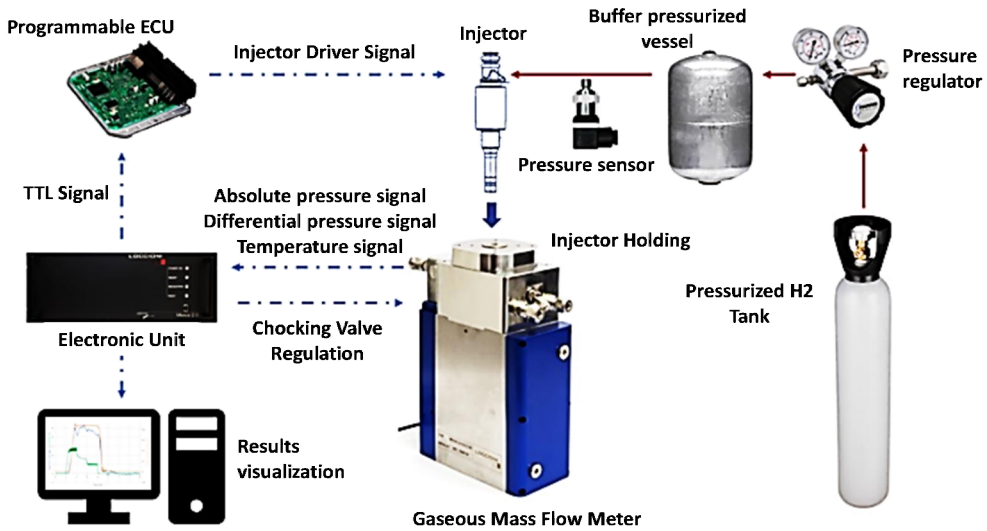

Figure 1 Layout of the experimental apparatus for the mass flow rate measurements

The gas supply system consists of a pressurized tank containing hydrogen connected to the injector via a line which includes the presence of a pressure regulator, a storage tank to reduce the gas pressure oscillations during the injection events, and a pressure sensor to collect the injection pressure just upstream the injector entrance.

For the present work, the injection rate measurements were realized through the Mexus AIR 2.0 device. This shot-to-shot device applies a variant of Zeuch's method to calculate the injection rate of a gas injector.

2-2- Spray Characterization Methodology

The injection process was studied by injecting hydrogen at room temperature into an optically accessible (80 mm in diameter) constant volume combustion vessel (CVCV) controlled in

temperature and pressure to replicate the typical thermodynamic engine conditions. The gas supply line was the same as described in the above paragraph. The injector was located in an ad-hoc adaptor on the vessel top so that the jet developed towards the vessel center in the radial direction. Schlieren optical technique was used to acquire the H_2 jet images for a wide range of engine-like conditions by a high-speed CMOS camera.

The desired ambient pressures were realized by delivering nitrogen inside the vessel. More details of the experimental apparatus can be found in [19]. A customized procedure developed in the C# environment with the help of some image-processing libraries was implemented to process the images and ensure adequate enhancement to allow the measurement of the jet macroscopic characteristics. Further details on the adopted image processing procedure were reported in [20, 21].

3- Results and Discussion

For confidentiality reasons agreed with the industrial partner, the trends relating to the mass flow rate measurements will not be reported in the paper. For the same reason, the curves relating to the axial penetrations and jet areas will be shown in a dimensionless way, not affecting the complete understanding of the jet behavior for the ambient and injection conditions.

The mass flow rate measurements were carried out for single injection strategies at different injection pressures (p_{inj}) and energizing time (ET) by keeping constant ambient pressure (p_{amb}). Table 1 summarizes all the tested conditions.

Table 1 Test plan for mass flow rate measurements

P_{inj} [bar]	P_{amb} [bar]	ET [bar]
20-30-40	3.0	1.25 – 2.25 – 3.0

The effects of the backpressure, established in the fuel meter, on the total delivered gas were studied by moving the ambient pressure from 3.0 to 4.5 bar. The results showed negligible differences indicating that, at the examined range, the flux of gas is largely independent of the pressure downstream of the nozzle.

Finally, Figure 2 reports the comparison of the total injected quantities vs the energizing times as a function of the pressure upstream at ambient pressure of 3.0 bar. The graphs well depict the linear and coherent behavior both concerning the injection pressures and injection durations. The effect of the injection pressure was well-scaled in terms of the total amount of injected fuel per stroke.

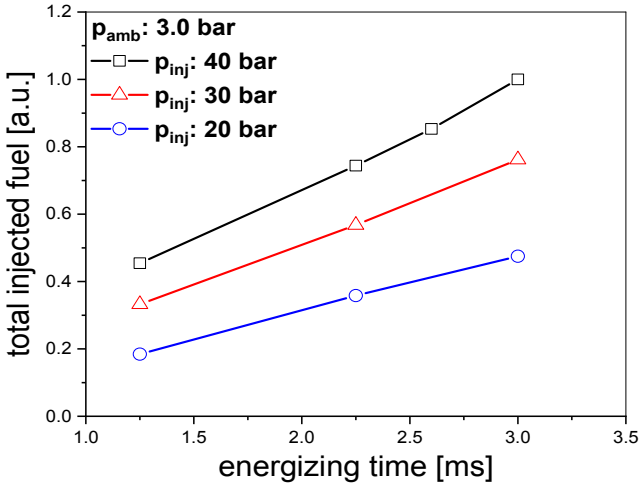

Figure 2 Total amount of injected fuel vs time at different injection pressures

3-1- Spray Morphology Characterization

In this study, schlieren visualizations were used to determine the macroscopic jet characteristics of H2 and its inner structure mainly in terms of gas spread, tip penetrations, and the shockwave formation inside a pressurized vessel. Table 2 summarizes all the tested conditions in terms of energizing time, injection, and ambient pressure. For each injection pressure, three ambient pressures were tested by keeping the energizing time at 2.6 ms.

Table 2 Test conditions for H_2 jet characterization

P_{inj} [bar]	P_{amb} [bar]	ET [bar]
20-30-40	3.0	1.25 – 2.25 – 3.0

Figure 3 depicts the volume occupied by the injected H2 in the vessel at the explored injection pressures of 20, 30, and 40 bar for different times from the start of injections (tSOI) and precisely 0.23, 0.59, 0,90, and 1.26 ms. The tSOI was considered as the first frame with the appearance of the fuel from the nozzle tip at each condition.

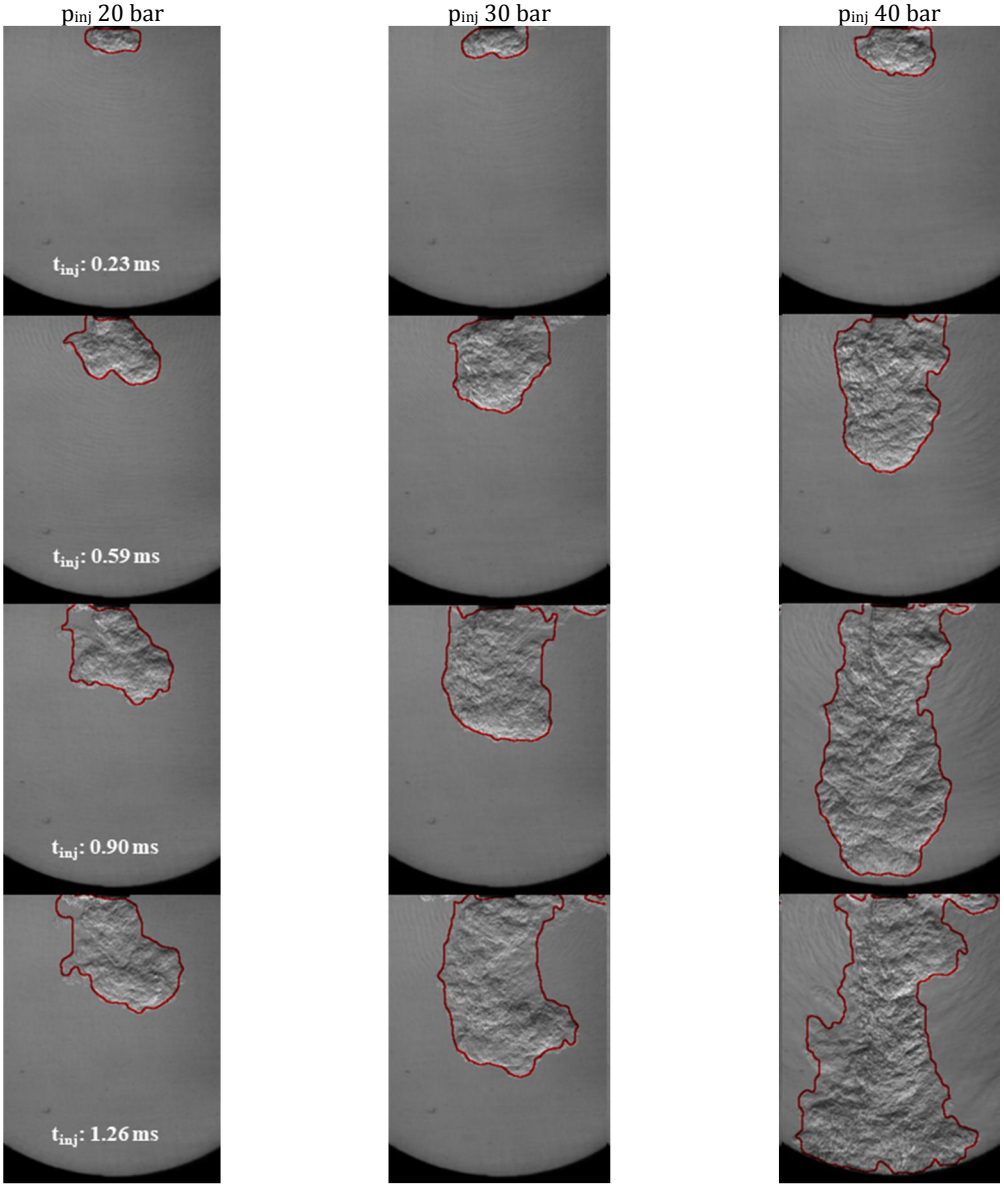

Figure 3 Effect of injection pressure on H2 jet morphology @ p_{amb} 4.5 bar

The injection duration was constant at all the conditions and resulted in 2.6 ms while the limit of penetration measurements was given by the quartz windows clearance. At this step of the work, no compressibility of the injected gas was considered as the first approximation being the backpressure constant equal to 4.5 bar even if different injected quantities due to diverse pressures are not free from compressibility effects. N2 gas was used to realize the desired ambient pressure at an ambient temperature of 276 K.

At equal time from the SOI (rows in Figure 3), the increase of the injection pressure translates to greater quantities of delivered fuel at higher momentum. In the approximation of negligible compressibility of the incoming gas, both the penetration of the tip of the spray and its widening appear evident at each of the reported times while shock waves, determined by the incoming of the H2, are highlighted since the first frame with more pronounced intensities at the increasing of the injection pressure. Anyway, the experimental technique and the appropriate image post-processing enabled a perfect definition of the fuel body concerning the chamber filling gas, although we are describing gas penetrating other gas. The red line permits to envelope of the H2 jet and facilitates the measure of the tip penetration. At a later time from the SOI (next rows), the solid-body structure of the spray penetrates the gas up to the window limit of our apparatus where no more increments are measurable. Inside the H2 jets, structures are due to different densities but, mainly, the Mach disks and Barrel shock structures appear, and we will deal with this later.

Figure 4 reports the behavior of the tip penetrations for the fixed injection pressures and backpressure of 4.5 bar. We considered the maximum extension as the limit of the optical window located on the high-pressure chamber and respect to it parametrized the behavior of the jet maximum extension.

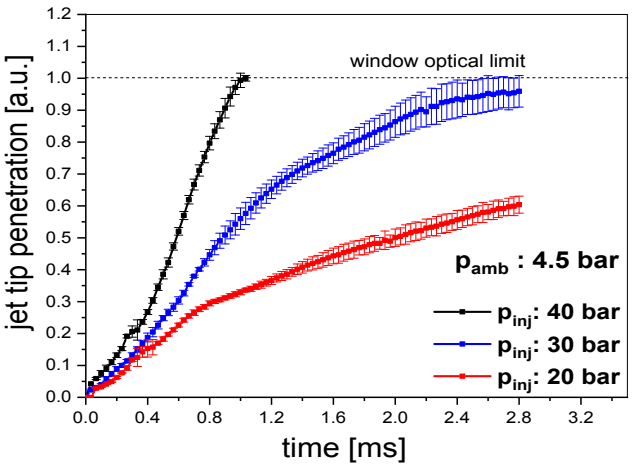

Figure 4 H2 jet penetration curves vs p_{inj} @ pamb:4.5 bar

Predictably, highest the injection pressure is and fastest the tip reaches this limit. In fact, at 40 bar (black curve) the tip is measurable up to 1.0 ms, while the blue and red curves, reporting the tips at 30 and 20 bar, respectively, never reach that limit during the entire injection event. Two further comments to the curves: the huge amount of data per each condition permitted a punctual and sequential reporting of the penetration behavior while the limited error bar heights, mainly at the early stages, give the repeatability of the event. Factor, this last one, already noted during the flow rate measures.

The “40 bar” curve shows a quasi-linear trend until reaching the optical limit. Vice versa, the “30 bar” curve shows an initial linear trend up to about one-third of its extensions where a change of slope appears denoting a variation in the trend in the sense of increasing. Finally, concerning the “20 bar” condition (red curve), an equivalent point seems existing around 25

% of the limit, after that the penetration curve assumes a log-type behavior typical of the jets under a non-negligible braking effect (like for liquid sprays).

Analogue behavior was carried out at other two ambient pressures with respect to the injection pressure variation, here not reported.

The behavior of the H2 jets injected in the N2 ambient gas was analyzed as a function of the backpressure values of 1.5, 3.0, and 4.5 bar. At these three p_{amb}, the images of the sprays were freezed at 0.561 ms from the SOI at the injection pressures of 20, 30, and 40 bar, Figure 5.

At the same tSOI, each row of the Figure 5 shows the H_2 volume occupancy in the chamber and how the penetrations decrease at the increasing of the N_2 pressure. The breaking effect of the gas density is instantly evident on jet morphology resulting in a shorter, larger, and denser jet with increasing of the N_2 pressure, at equal injection pressure.

Characteristics and well visible shock waves, generated by the propagating sprays, were detected at the highest backpressure. The Mach disks at the exit of the nozzle were well evident at the highest net pressure ratios (NPR) meaning a combination of low p_{amb} and high p_{inj}. They will be described in the next paragraph.

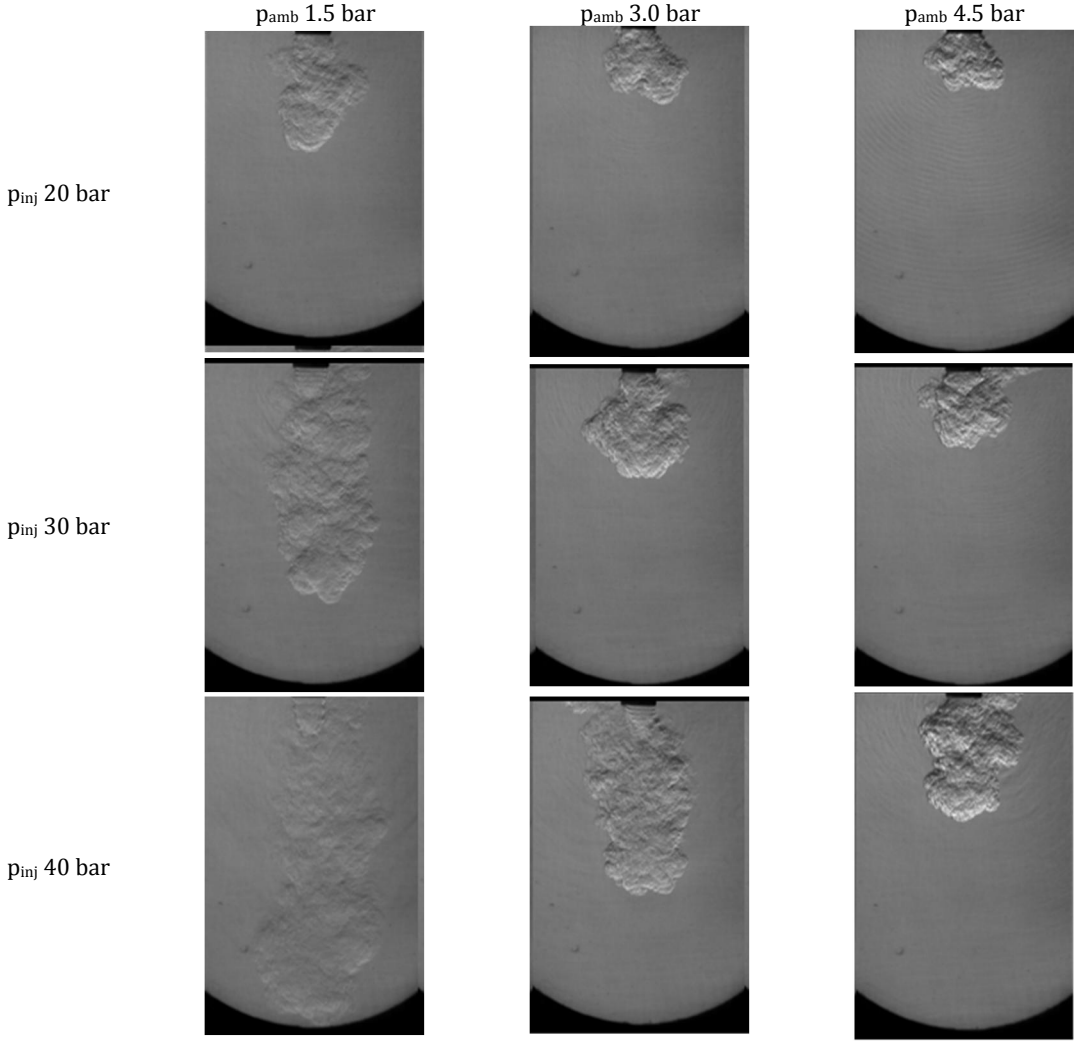

Figure 5 Effect of ambient pressure on H2 jet morphology @ t_{inj}:0.561 ms

Figure 6 reports the trend of the jet tip penetrations for the ambient pressures of 1.5, 3.0, and 4.5 bar remaining constant the injection pressure at 30 bar. The window optical limit is quickly reached at the lowest backpressure of 1.5 bar at 0.80 ms after the SOI due

to the lowest effect of the filling brake in the combustion vessel. At increasing of backpressures, the "3.0 bar" condition extends the H2 penetration up to 1.60 ms from the SOI (blue curve) while the "4.5 bar" one never permitted the window limit reaching all along the injection duration exercising an effective braking force on the fuel progress. At 2.8 ms from the SOI, with the injector now closed, the total penetration is around 95 %.

As well as in Figures 4, the huge amount of measured points and the excellent indetermination bars on them give the filling of the repeatable behavior of the injector and the correctness of the trend described.

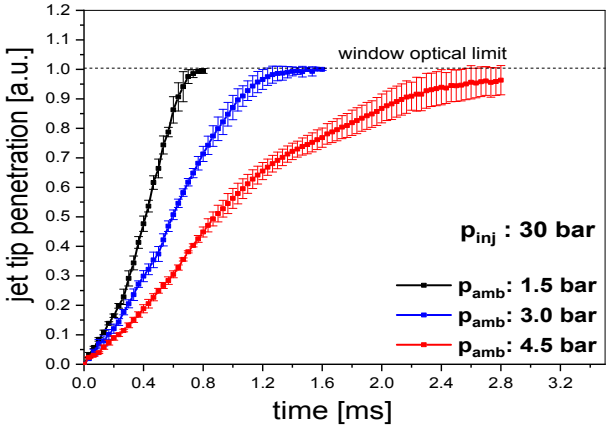

Figure 6 H_2 jet penetration curves vs p_{amb} @ p_{inj} 30 bar

To further study the effects of the injection pressure on H2 jet morphology, the jet areas were also measured for all the investigated conditions. The areas are the total surfaces included in the red contours (Figure 3) measured as the number of pixels. The calibration factor, of 5.48 pixel/mm, allowed to calculate the actual surfaces of the images in mm2. The Figure 7 depicts the spreading of the gaseous fuel at the varying of the ambient pressure at injection pressure of 30 bar. It is clearly visible the effect of the ambient density generating trends just like the ones refer to penetrations reported in Figure 6 for the same injection conditions. At early stages the curves (Figure 7) overlap, later each one proceeds with a growing trend over time and which values are inversely proportional and well-scaled with the ambient pressures. As well as for the results reported in Figure 6, the areas related to the conditions of 1.5 and 3.0 bar as ambient pressure were measured up to the jet reached the optical limit of the window. Similar behaviors, here not reported, were registered for the other injection pressures (20 and 40 bar) versus the ambient pressures. Summarizing, the results showed a pronounced effect of the ambient pressure on jet morphology generating a clear contraction in terms of both axial penetration and global jet area with increasing of the ambient pressure because of the compressibility of the gas.

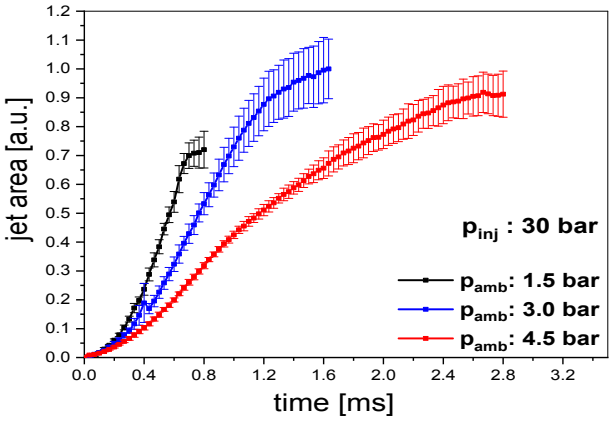

Figure 7 Ambient pressure effect on the H_2 jet area @ p_{inj}:30bar

3-2- Barrel shock structure and the Mach disk

When a compressible fluid is injected at high pressure into the combustion chamber, choked flow conditions can occur in the exit section of the nozzle (as well inside it), resulting in the formation of shock waves and discontinuities that influence the process mixing in the downstream area. The formation of these under-expanded structures, recognizable by the presence of “barrel shock” in the structure of the jet, depends mainly on the ratio between the pressure upstream of the injector nozzle (p_{inj}) and the pressure inside the cylinder (p_{amb}), defined "net pressure ratio" (NPR) [21, 22]. The jet undergoes an evolution of its structure passing from subsonic to moderately under-expanded up to strongly under-expanded with appearance of Mach disk.

In this section, the evolution of the shockwave structure was described under highly expanded spray conditions (NPR ≥ 4) in terms of Mach disk height (H). Figure 8 shows the variation of the Mach disks height at the varying of the NPR when the jet is completely developed, 825 μs after the start of injection, and the “H” value is almost constant. Different NPRs were realized by keeping constant the injection pressure at 40 bar resulting values of the NPR of 26.6, 13.3, and 8.9 for the ambient pressures of 1.5, 3.0, and 4.5 bar, respectively.

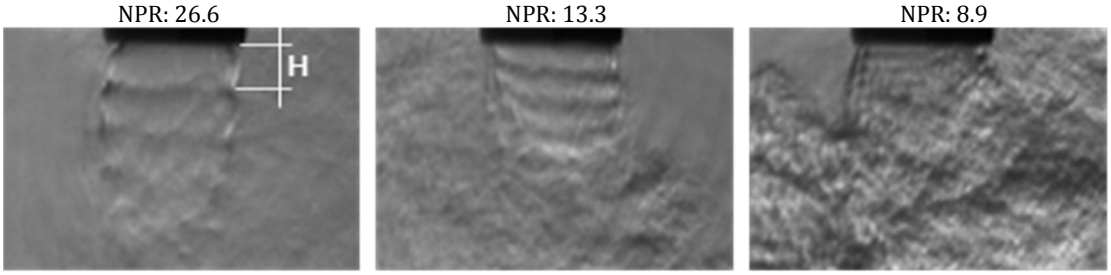

Figure 8 Effect of the NPR on Mach disk variation @ p_{inj} 40 bar

The Mach disk structure was resolved for the near-field region and denoted through its height (H). It was defined (Figure 8) as the maximum distance from the nozzle exit to the first Mach disk location and it demonstrated a strong dependence by the NPR.

Figure 9 reports the Mach disk heigh evolution (H) for different NPRs at the injection pressure of 40 bar. Per each profile, the zero-time was normalized with respect to the instant where the first Mach disk appears since a light delay was collected with decreasing of the NPR (less than 0.3 ms between 26.6 and 8.9 values).

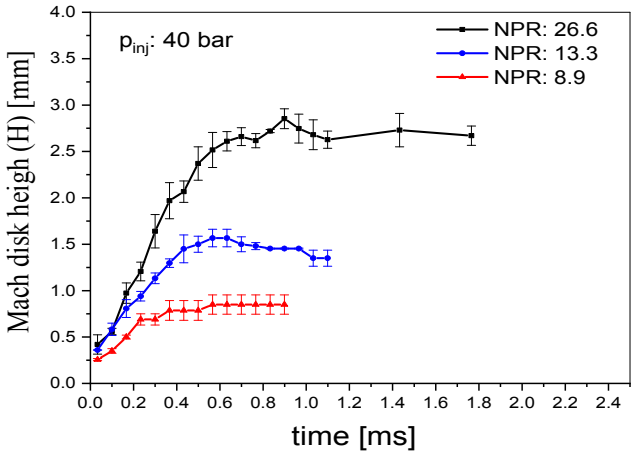

Figure 9 Effect of NPR on the Mach disks height

Each profile presents a formation phase, in which an increase in the height of the Mach disk was found, until reaching a rather stable value, indicating that the pressure upstream the nozzle stabilized, after a time strongly dependent on the NPR value: about 0.3, 0.5, and 0.7 ms at 8.9, 13.3, and 26.6 as NPR, respectively. The quasi-stable value was strongly affected by the NPR varying from 2.7 to 0.7 mm, approximately, by moving the NPR from 26.6 and 8.9. Finally, for longer times, here not reported but collected from jet imaging processing, the disks height gradually decreases following the closure of the injector.

4- Conclusions

In this study, high-pressure hydrogen jet behavior was carried out in terms of mass flow rate measurements and morphology investigation under a wide range of engine-like conditions. Macroscopic jet parameters were measured to study the H2 jet morphology under a wide range of ambient and injection conditions. Measures of Mach disc heights were instead considered to characterize the shockwave structure. The main conclusions are listed as follow:

- The adopted device for the gaseous mass flow rate measurements has proven capable of studying the pneumatic behavior of the injector with a high degree of reliability for all the investigated conditions. Mass flow rate measurements showed negligible effects on mass flux from varying the backpressure from 3.0 to 4.5 bar at the same injection pressure and energizing time, while a strong dependence from injection pressure and duration was registered.
- Higher gas injection pressures resulted in higher jet tip penetration. The highest values of the penetration were detected with increased fuel injection pressure when the ambient pressure was the lowest one. Vice versa, the effects of injection pressure look negligible on jet cone angle variations. The main effect of the injection gas pressure increase was the growth of the injected fuel and consequently of the occupied volume from the H2 jet, keeping constant (2.6 ms) the energizing time. As consequence, at the equal ambient pressure, the spray looks longer and less dense.
- Strong effects of the ambient pressure were carried out on jet evolution resulting in decreasing of both tip penetration and jet area with increasing of the ambient pressure for all the investigated injection pressures. More, due to the compressibility of the gas, the local density inside the jet increased with increasing of ambient pressure.
- For each of the injection pressures, the jet undergoes an evolution of its structure passing from subsonic to moderately under-expanded up to strongly under-expanded with appearance of Mach disks. The height of the Mach disks increased during the initial phases, after that it reached a quasi-stable value with a pronounced inverse trend with respect to the injection and ambient pressure ratio (NPR).

In conclusion, the illustrated results aim to improve the knowledge of under-expanded jets evolution under a wide range of injection and ambient conditions and could be useful to provide a robust data set to develop advanced CFD numerical models.

Acknowledgment

The authors would like to gratefully thank PHINIA company to supply the hydrogen injector used in the present research activity.

List of Symbols

Compressed Hydrogen Gas	*CHG*
Carbon monoxide	*CO*
Direct Injection	*DI*
Constant Volume Combustion Vessel	*CVCV*
Energizing Time	*ET*
Greenhouse Gases	*GHG*
Mach disk height	*H*
Internal Combustion Engine	*ICE*
Nitrogen Oxides	*NOx*
Net Pressure Ratio	*NPR*
Port Fuel Injection	*PFI*
Injection pressure	*pinj*
Ambient pressure	*pamb*
Time Start of Injection	*tSOI*
Root Mean Square	*RMS*
Research Octane Number	*RON*

References

[1] Bouckaert S, Pales AF, McGlade C, Remme U, Wanner B, Varro L, D'Ambrosio D, Spencer T. Net zero by 2050: A roadmap for the global energy sector. 2021.

[2] Dilara P. The future of clean cars in Europe: EU Green Deal and EURO 7. InSino-EU Workshop on New Emissions Standards and Regulations for Motor Vehicles 2021 Jan 25.

[3] Stępień Z. A comprehensive overview of hydrogen-fueled internal combustion engines: Achievements and future challenges. Energies. 2021 Oct 11;14(20):6504. doi: 10.3390/en14206504

[4] Manoharan Y, Hosseini SE, Butler B, Alzhahrani H, Senior BT, Ashuri T, Krohn J. Hydrogen fuel cell vehicles; current status and future prospect. Applied Sciences. 2019 Jun 4;9(11):2296. doi: 10.3390/app9112296

[5] Hosseini SE, Butler B. An overview of development and challenges in hydrogen powered vehicles. International journal of green energy. 2020 Jan 2;17(1):13-37. doi: 10.1080/15435075.2019.1685999

[6] Dougherty W, Kartha S, Rajan C, Lazarus M, Bailie A, Runkle B, Fencl A. Greenhouse gas reduction benefits and costs of a large-scale transition to hydrogen in the USA. Energy policy. 2009 Jan 1;37(1):56-67.

[7] Yip HL, Srna A, Chun Yin Yuen A, Kook S, Taylor RA, Heng Yeoh G, Medwell PR, Chan QN. A review of hydrogen direct injection for internal combustion engines: Towards carbon-free combustion. Appl. Sci. 2019, 9, 4842. doi: 10.3390/app9224842

[8] Verhelst S, Wallner T. Hydrogen-fueled internal combustion engines. Progress in energy and combustion science. 2009 Dec 1;35(6):490-527.

[9] Teoh YH, How HG, Le TD, Nguyen HT, Loo DL, Rashid T, Sher F. A review on production and implementation of hydrogen as a green fuel in internal combustion engines. Fuel. 2023 Feb 1;333:126525. doi: 10.1016/j.fuel.2022.126525

[10] Dash SK, Chakraborty S, Roccotelli M, Sahu UK. Hydrogen fuel for future mobility: Challenges and future aspects. Sustainability. 2022 Jul 6;14(14):8285. doi: 10.3390/su14148285

[11] Bekdemir C, Doosje E, Seykens X. H2-ICE Technology Options of the Present and the Near Future. SAE Technical Paper; 2022 Mar 29. doi: 10.4271/2022-01-0472

[12] Matthias NS, Wallner T, Scarcelli R. A hydrogen direct injection engine concept that exceeds US DOE light-duty efficiency targets. SAE International Journal of Engines. 2012 Aug 1;5(3):838-49.

[13] Mohammadi A, Shioji M, Nakai Y, Ishikura W, Tabo E. Performance and combustion characteristics of a direct injection SI hydrogen engine. International Journal of Hydrogen Energy. 2007 Feb 1;32(2):296-304. doi: 10.1016/j.ijhydene.2006.06.005

[14] Oikawa M, Ogasawara Y, Kondo Y, Sekine K, Takagi Y, Sato Y. Optimization of hydrogen jet configuration by single hole nozzle and high speed laser shadowgraphy in high pressure direct injection hydrogen engines. International Journal of Automotive Engineering. 2012;3(1):1-8.

[15] Yip HL, Srna A, Yuen AC, Kook S, Taylor RA, Yeoh GH, Medwell PR, Chan QN. A review of hydrogen direct injection for internal combustion engines: towards carbon-free combustion. applied sciences. 2019 Nov 12;9(22):4842. doi: 10.3390/app9224842

[16] Takagi Y., Mori H., Mihara Y., Kawahara N., Tomita E., "Improvement of thermal efficiency and reduction of NOx emissions by burning a controlled jet plume in high-pressure direct-injection hydrogen engines", Int J Hydrogen Energy 2017; 42(41); 26114-26122, doi: 10.1016/j.ijhydene.2017.08.015

[17] Faizal M, Chuah LS, Lee C, Hameed A, Lee J, Shankar M. Review of hydrogen fuel for internal combustion engines. J. Mech. Eng. Res. Dev. 2019 Apr;42(3):36-46. doi: 10.26480/jmerd.03.2019.35.46

[18] Dober G, Hoffmann G, Piock WF, Doradoux L, Meissonnier G, Ouali E. An Efficient Path to Zero CO_2 Powertrains–BorgWarner's Hydrogen Injection Systems, in Internationales Wiener Motorensymposium, Vienna, Austria, 2022.

[19] Duronio F, De Vita A, Allocca L, Montanaro A, Ranieri S, Villante C. CFD numerical reconstruction of the flash boiling gasoline spray morphology. SAE Technical Paper; 2020 Sep 27. doi: 10.4271/2020-24-0010

[20] Montanaro A, Allocca L, De Vita A, Ranieri S, Duronio F, Meccariello G. Experimental and numerical characterization of high-pressure methane jets for direct injection in internal combustion engines. SAE Technical Paper; 2020 Sep 15. doi: 10.4271/2020-01-2124

[21] Allocca L, Montanaro A, Meccariello G, Duronio F. et al., "Under-Expanded Gaseous Jets Characterization for Application in Direct Injection Engines: Experimental and Numerical Approach, SAE Technical Paper 2020-01-0325, 2020 Apr 14. doi: 10.4271/2020-01-0325

[22] Pham Q, Chang M, Kalwar A, Agarwal AK, Park S, Choi B, Park S. Macroscopic spray characteristics and internal structure studies of natural gas injection. Energy. 2023 Jan 15;263:126055. doi: 10.1016/j.energy.2022.126055

نشریه علمی تحقیقات موتور
زمستان ۱۴۰۲، جلد ۷۰، شماره ٤، صفحه ۲۷-۳۹
تارنمای نشریه: www.engineresearch.ir

مقاله پژوهشی

خصوصیات فواره هیدروژن فشار بالا برای موتور احتراق داخلی از نظر مورفولوژی و نرخ جریان

الساندرو مونتانارو*، لوئیجی آلوکا، جیووانی مکاریلو

موسسه علوم و فناوری‌های انرژی تجدیدپذیر، شورای تحقیقات ملی، ایتالیا

اطلاعات مقاله

کلیدواژه‌ها:
تزریق هیدروژن
تزریق مستقیم
سوخت گازی

چکیده

سوختن سوخت‌های سنگواره‌ای در موتورهای احتراق داخلی که منجر به حجم عظیمی از گازهای گلخانه‌ای (GHG) و افزایش شدید دمای جهانی می‌شود، دلایل سختگیرانه‌تر شدن قوانین آلایندگی برای حفاظت از سلامت هستند که تحقیقات بیشتر در مورد سوخت‌های جایگزین را تشویق می‌کنند. در این راستا، هیدروژن به دلیل ماهیت کربن صفر آن، به عنوان یکی از سوخت‌های بالقوه پاک در نظر گرفته شده است. توسعهٔ فعلی موتورهای احتراق داخلی مبتنی بر هیدروژن بر راهبرد تزریق مستقیم (DI) متمرکز است زیرا باعث می‌شود بازده موتور بهتری نسبت به تزریق سوخت در راهگاه داشته باشد. رفتار فواره سوخت یک جنبه اساسی از نسبت اختلاط هوا به سوخت درون استوانه است که بر فرآیند احتراق، عملکرد موتور و انتشار آلاینده‌ها تأثیر می‌گذارد. در مطالعه حاضر، بررسی‌های جامعی در مورد رفتار فواره هیدروژن تولید شده توسط یک افشانه گاز هیدروژن فشرده شده (CHG) تحت شرایط مختلف عملیاتی، انجام شد. یک سامانه اندازه‌گیری مناسب برای سوخت‌های گازی برای اندازه‌گیری نرخ جریان استفاده شد. ریخت‌شناسی فواره سوخت در یک مخزن با حجم ثابت پر از ازت به عنوان تابعی از فشار تزریق (تا ۴٫۰ مگاپاسکال) و فشار برگشتی متفاوت در ظرف، از طریق اندازه‌گیری نفوذ فواره، کل مساحت و زوایای مخروط که وابستگی شدید به متغیرهای تنظیم شده را نشان می دهد مطالعه شد. روش تصویربرداری شلیرن حل شده با چرخه توسط دوربینی با سرعت تند برای پیگیری گسترش فواره استفاده شد، در حالی که تصاویر توسط یک روش ساخت خانگی پردازش شدند، اجازه شناسایی خطوط فواره هیدروژن در گاز ازت و در نتیجه اندازه‌گیری متغیرهای اصلی مشخص کننده ساختار فواره فراهم شد.

* نویسنده مسئول
پست الکترونیکی: alessandro.montanaro@stems.cnr.it (الساندرو مونتانارو)

دریافت ۲۹ اردیبهشت ۱۴۰۳؛ پذیرش ۴ خرداد ۱۴۰۳
شاپای الکترونیکی: ۴۱۲۱-۲۳۴۵ / شاپای چاپی: ۵۲۱۴-۱۷۳۵

Cite this article: Montanaro A, Allocca L, Meccariello G. Characterization of High-pressure Hydrogen Jet for ICE in terms of Morphology and Flow-rates. The Journal of Engine Research. 2024 Feb 20;70(4):27-39. doi: 10.22034/ER.2024.2029585.1054